1-1-2017

Effect of Water Hardness on Adsorption of Lead from Aqueous Solution using Douglas Fir Biochar

Dhara Gogri

Effect of water hardness on adsorption of lead from aqueous solutions using Douglas fir biochar

By

Dhara Gogri

A Thesis
Submitted to the Faculty of
Mississippi State University
in Partial Fulfillment of the Requirements
for the Degree of Master of Science
in Chemistry
in the Department of Chemistry

Mississippi State, Mississippi

August 2017

Effect of water hardness on adsorption of lead from aqueous solutions using

Douglas fir biochar

By

Dhara Gogri

Approved:

Todd E. Mlsna
(Major Professor)

David O. Wipf
(Committee Member)

Debra Ann Mlsna
(Committee Member)

Joseph P. Emerson
(Graduate Coordinator)

Rick Travis
Dean
College of Arts & Sciences

Name: Dhara Gogri

Date of Degree: August 11, 2017

Institution: Mississippi State University

Major Field: Chemistry

Major Professor: Todd E. Mlsna

Title of Study: Effect of water hardness on adsorption of lead from aqueous solutions using Douglas fir biochar

Pages in Study: 47

Candidate for Degree of Master of Science

Water pollution due to heavy metals can be hazardous to both the environment and human health. The aim of this research is to provide a low-cost alternative for lead remediation. Biochar was produced from the fast pyrolysis of Douglas fir (DBC). Magnetic biochar (MDBC) was synthesized by mixing aqueous biochar suspensions with an aqueous $Fe^{3+/}Fe^{2+}$ solution.

In chapter I, an overview of lead as an emergent contaminant is given. Different biochar production techniques have been discussed along with different mechanism of adsorption of lead onto biochar.

Chapter II is a study of adsorption of lead on DBC and MDBC under different experimental conditions. The main aim of this research is to study the effect of water hardness on adsorption capacity. Three levels of water hardness were employed. Sorption performances were evaluated using Langmuir and Freundlich adsorption isotherms. DBC and MDBC were also successfully applied for lead removal from natural water samples.

In chapter III, future projects focused on studying the effects of matrix chemicals found in natural waters on the heavy metal ion adsorption properties of biochar are discussed.

DEDICATION

I would like to dedicate this thesis

To my mother Trupti Gogri

for all her love and enormous support

To my father Arvind Gogri

For supporting and encouraging me to believe in myself

ACKNOWLEDGEMENTS

Firstly, I would like to express my sincere appreciation to my advisor Dr. Todd Mlsna for the continuous support, encouragement, and immense knowledge. His guidance helped me all the time. I would also like to express my gratitude to the members of my graduate committee, Dr. David O. Wipf, and Dr. Deb Mlsna, for their advice and guidance.

Also, I would like to thank my fellow lab mates: Achala, Akila, Narada, and Griffin for their help and support towards the successful completion of my Master's program. And special thanks to my wonderful undergraduate researcher Harshini who assisted me in my experiments.

I would also like to thank Hellen and Randika for making my graduate life more bearable and often, fun.

Finally, I must express my very profound gratitude to my parents, my sister Dhvani and to my boyfriend Kunal for providing me with unfailing support and continuous encouragement throughout my years of study and through the process of researching and writing this thesis. This accomplishment would not have been possible without them.

TABLE OF CONTENTS

LIST OF TABLES

LIST OF FIGURES

CHAPTER I

INTRODUCTION

1.1 Water pollution

More than two-thirds of Earth's surface is covered by water; less than a third is taken up by land. Only a small fraction of the earth's water is both fresh and available for human use and as the Earth's population continues to rise, so does pressure on the planet's water resources. Water pollution due to heavy metals,[1] pesticides,[2] disinfectants,[3] pharmaceuticals[4] and dyes[5] also increases with population growth, therefore, clean water is a valuable, and increasingly scarce, natural resource.[6]

Lead is emerging as one of the most common heavy metal water pollutant. Lead is a non-essential and toxic metal with no known biological benefit to humans. The main anthropogenic sources of lead in aquatic environments are fossil fuel combustion,[7] mining,[8] refining of ores[9] and the use of gasoline containing lead[10] (now banned in all but 6 nations). Lead can also enter natural water systems naturally from direct exposure to rocks and soils[11] and can enter drinking water supplies when service pipes that contain lead corrode[12].

Lead is environmentally persistent and can bioaccumulate in the body over time.[13] In adults, inorganic lead does not penetrate the blood–brain barrier, whereas this barrier is less developed in children. High gastrointestinal uptake and the permeable blood–brain barrier make children especially susceptible to lead exposure and subsequent brain

damage.[14] The maximum allowable content of lead in drinking water, as set by the U.S. Environmental Protection Agency, is 15 ppb. Ninety percent of water samples taken in Flint, Michigan from 2014 to 2016 had lead levels above 25 ppb. Therefore, developments of methods for removal of lead from water systems is crucial. Common methods employed for aqueous Pb^{2+} removal include chemical precipitation,[15] ion-exchange,[16] membrane processes,[17] solvent extraction[18] and electrodeposition[19]. These techniques can be expensive and time consuming.

1.2 Adsorption technology

Adsorption is a fast, inexpensive and universal method used to remediate heavy metals and other pollutants.[20] Several adsorbents including activated carbon,[21] clay,[22] minerals,[20] and zeolites[23] have been applied for Pb^{2+} removal. Activated carbon is the most common adsorbent used because of its high surface area, thermal stability, porous structure, and wide pH application range. Despite these advantages, its powdered form is not easily separated from the solution and it has high production costs.[24] Therefore, the search for inexpensive, readily available and easily regenerated adsorbents is important.

1.3 Biochar

Biochar has been defined by Lehmann and Joseph as "a carbon (C)-rich product when biomass such as wood, manure or leaves is heated in a closed container with little or no available air".[25] In recent years, biochar has received increasing attention due to its multi-functionality including carbon sequestration,[26] bio-energy,[27] soil fertility enhancement,[26] and environmental remediation.[28] The sum of extensive research confirms biochar's excellent ability to immobilize organic[28] and inorganic pollutants[29] in

soil and water systems. Inorganic pollutants, mainly heavy metals can be passed along the food chain through bioaccumulation as they are non-biodegradable. Biochar is considered to be an alternative in water treatment technology for metal removal. It is a less expensive alternative to activated carbon and is often formed as a byproduct of the bio-fuel industry.

An innovative adsorption method for wastewater treatment is the use of magnetic biochar, which can be used in batch, stirred-tank processes and recovered with a magnet.[30-31] Small particle size increases often improve a materials adsorption properties, however, filtration becomes very slow, as adsorbent particle size decreases. Thus, simple magnetic field separation could allow for practical use of small particle size adsorbents which have high surface areas and faster adsorption kinetics.

1.3.1 Biochar production techniques

The physical and chemical properties of biochars vary depending on biomass source, production method, and post- and pretreatments. Biochar can be produced from a wide range of feedstock materials, agricultural and forest residues,[32] and industrial by-products and wastes.[33] Biochar can be prepared via thermal or biological routes,[34] with thermal processing being the most common method. Pyrolysis (slow or fast),[35] gasification,[36] and torrefaction[37] are a few examples of thermal processes.

1.3.1.1 Biomass pyrolysis

Pyrolysis (slow or fast) is the thermal decomposition of materials in the absence of oxygen or in the presence of a smaller amount of oxygen than is required for complete combustion.[35-36] Solids (chars), liquids, and gasses are produced during the process. The

composition of the product depends on the production conditions including temperature, heating rate, and residence time in the hot zone. In slow pyrolysis, biomass is heated slowly to about 500 ºC in the absence of air. Biochar yields from slow pyrolysis are between 25-30%.[38] Fast pyrolysis typically uses feedstock with less than 10% moisture, temperature increases to 400-900 ºC and a residence time of around 2 s. The main product of fast pyrolysis is bio-oil with biochar yields ranging from 12-26%.[38]

1.3.1.2 Gasification

Gasification is the partial combustion of a solid in the presence of air or steam at elevated temperature, typically between 600 to 1400 ºC to produce primarily bio-syngas, bio-oil and biochar.[37] The composition of the product mixture depends on temperature, particle size, residence time, pressure, and gas composition under which the biomass is treated. The partial combustion of the biomass is achieved by administering a controlled amount of oxygen into the reaction chamber. The main gasses produced are carbon monoxide, carbon dioxide, and hydrogen. Gasification produces a significant quantity of the syngas product but typically less than 10 % of biochar[38]

1.3.1.3 Torrefaction

Torrefaction is a thermochemical method in which the biomass material is heated under atmospheric pressure between 200 to 320 ºC in the absence of oxygen.[37] Torrefaction increases biomass energy density, enhances hydrophobicity and greatly reduces weight. It does not create adsorbent chars but torrefied biomass (a brown or black product). The process results in partial decomposition which prevents rot of the biomass and induces some water loss.

Table 1.1 Average solid product yield from different biomass processing methods

Process type	Temperature °C	Biochar yields (in mass %)	References
Torrefaction	~300	61-84%	[37]
Slow pyrolysis	~400	25-30%	[35,36]
Fast pyrolysis	~800	12-26%	[35,36]
Gasification	~1000	≈ 10%	[36]

1.3.2 Biochar adsorption mechanism

Different interactions may take place between the biochar surface and the metal. Mechanisms controlling the removal of heavy metals from aqueous solutions include physical sorption, ion exchange, electrostatic interactions, complexation, and precipitation.[39]

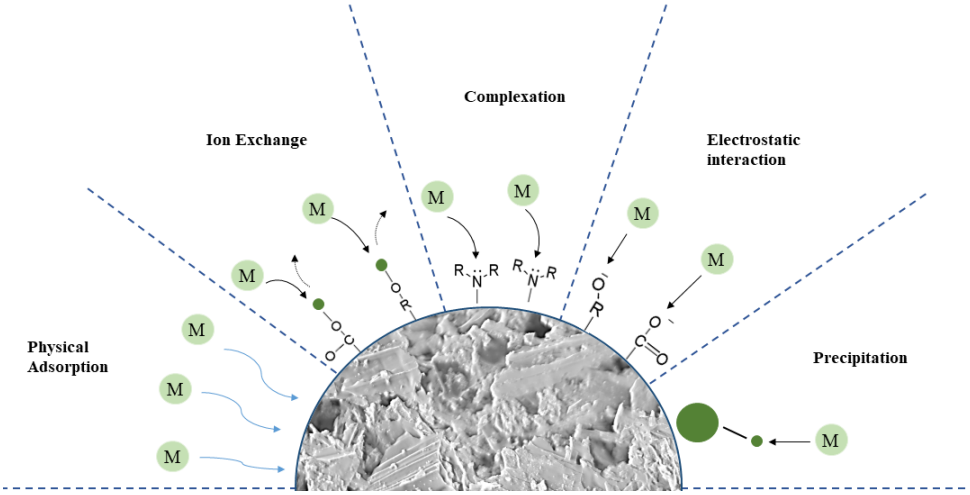

Figure 1.1 Metal adsorption mechanism onto biochar surface

Interactions include ion exchange, electrostatic attraction, surface complexation, physical adsorption, and co-precipitation[39]

1.3.2.1 Physical sorption

Physical sorption describes the removal of heavy metals by diffusional movement of metal ions into the biochar pores without the formation of chemical bonds.[40] Phenomena associated with van der Waals' forces can be included in this category.

1.3.2.2 Ion exchange

Sorption of heavy metals from aqueous solutions can occur from a selective replacement of positively charged ions on the biochar surface with target metal ions.[41] The efficiency of the ion exchange process is dependent on the size of the metal contaminant and the surface group chemistry of the biochar. The ionic radii, charge differences, and bond characteristics also determine the extent of exchange. Ions like K^+, Na^+, Ca^{2+}, and Mg^{2+} in biochar are responsible for the metal ion exchange with heavy metal ions such as Pb^{2+}, Cd^{2+}, Zn^{2+}, and Hg^+.

1.3.2.3 Electrostatic interactions

Metal removal from solution through electrostatic interaction between charged surface biochars and metal ions is another possible mechanism.[42] Biochar surfaces contain functional groups like carboxylic acid and hydroxyl groups; these groups can interact with metal ions using electrostatic interactions. This process is, however, dependent on the solution pH and point of zero charge.

1.3.2.4 Complexation

The metal removal from solution can also take place through complex formation on biochar surface after interaction between metal and active groups.[43] The amine groups in the biochar can form strong chemical bonds with metal ions enhancing adsorption. Metal ions can bind to unidentate ligands or through chelation.

1.3.2.5 Precipitation

Precipitation is one of the main mechanisms responsible for the immobilization of heavy metals by biochar through the formation of solid(s) on the biochar surface or the solution.[44] A biochars' mineral components like CO_3^{2-}, or PO_4^{3-} add extra surface adsorption sites and can form metal phosphate and metal carbonate precipitates. Less soluble forms of these mineral components exist at higher temperatures, and are more likely to be slowly released during the sorption process with heavy metals to form precipitates on a biochar surface.

1.4 Water hardness

As water moves through soil and rock, it dissolves very small amounts of minerals and holds them in solution. Ca^{2+} and Mg^{2+} dissolved in water are the two most

common minerals that make water "hard". The degree of hardness becomes greater as the calcium and magnesium content increases. General guidelines for classification of waters are: 0 to 60 mg/L (milligrams per liter) is classified as soft; 61 to 120 mg/L as moderately hard; 121 to 180 mg/L as hard; and more than 180 mg/L as very hard. The chemical form of metal ions is governed by physicochemical factors like salinity, pH, and hardness that prevail in the local environment. Water hardness is an important factor which can modify the environmental fate and adsorption of heavy metals in the natural environment.

1.5 Thesis objective

Wastewater pollution by heavy metal contaminants has become a subject of intense discussion. Removing these contaminants from aqueous solution is extremely important to improve water quality for both humans and animal consumption. Biochar is proposed as an alternative to traditional adsorption techniques using activated carbon. Biochar not only has an advantage of low-cost but also shows a promising removal capacity when used as an adsorbent to remove heavy metal contaminants in wastewater treatment.

Thousands of research articles have been published that detail the adsorptive properties of biochar. These studies have been done, almost exclusively, using a low concentration pollutant dissolved in distilled water. This approach typically results in significantly greater pollutant adsorption onto the biochar compared to the same concentration of pollutant in natural waters. The goal of this thesis is to begin the process of characterizing the effect of matrix chemicals found in natural waters on the heavy metal ion adsorption properties of biochar. The specific aim of this work is to understand

the properties of Douglas fir biochar and magnetic Douglas fir biochar for the adsorption of lead in different levels of water hardness.

CHAPTER II

LEAD REMEDIATION FROM HARD WATER USING MAGNETIZED AND NONMAGNETIZED DOUGLAS FIR BIOCHAR

2.1 Abstract

Biochar was produced from the fast pyrolysis of Douglas fir (DBC). Magnetic biochar (MDBC) was synthesized by mixing aqueous biochar suspensions with an aqueous $Fe^{3+/}Fe^{2+}$ solution, followed by NaOH treatment, which causes precipitation of magnetite, Fe_3O_4 onto DBC. The DBC and the resulting MDBC were investigated as potential green adsorbents for lead remediation from the water. The surface chemistry of both chars was examined by SEM, SEM-EDX, TEM, PZC, and surface area measurements. Batch sorption studies were carried out at 25 ºC, from pH 2-7 and with adsorbate concentration range of 50-200 mg/L. Maximum lead removal due to adsorption occurred at pH 5 for both DBC and MDBC. DBC was removed using filtration, whereas MDBC was removed magnetically. Remediated solutions were analyzed using atomic adsorption spectroscopy (AAS). Lead batch sorption studies were also conducted to study the effect of water hardness on rate and equilibrium data at different adsorbate concentrations to construct equilibrium isotherms. Three levels of water hardness were employed; low (30 mg/L), medium (90 mg/L) and high (150 mg/L). Sorption performances at 25 ºC were evaluated using Langmuir and Freundlich adsorption isotherm models. The maximum Langmuir adsorption capacity at pH 5 and 25 ºC for

low, medium and high hard water were 106.54, 85.65 and 76.70 mg/g for DBC and 69.93 mg/g, 64.88 mg/g and 63.03 mg/g for MDBC. DBC and MDBC were also successfully applied for lead removal from natural water samples. Both chars can be used as potential low-cost green adsorbents for lead remediation.

2.2 Introduction

Waste water pollution by lead is reported throughout the world as a major environmental concern. Lead is a non-essential and toxic metal with no known biological benefit to humans. Therefore, the US Environmental Protection Agency (EPA) has set the lead standards to less than 0.015 mg/L for drinking water. The main anthropogenic sources of lead in aquatic environments are fossil fuel combustion,[7] mining,[8] refining of ores[9] and the use of gasoline containing lead[10] (now banned in all but 6 nations). In adults, inorganic lead does not penetrate the blood–brain barrier, whereas this barrier is less developed in children. High gastrointestinal uptake and the permeable blood–brain barrier make children especially susceptible to lead exposure and subsequent brain damage.[14]

Adsorption is a fast, inexpensive and universal method used to remediate heavy metals and other pollutants.[20] Biochar is an adsorbent often formed as a byproduct of the bio-fuel industry and is often less expensive than activated carbon. Biochars ability to adsorb metals has been extensively studied. An innovative adsorption method for wastewater treatment is the use of magnetic biochar, which can be used in batch, stirred-tank processes and recovered with a magnet.[30-31]

Water forms complex chemical solutions. "Pure" water essentially is nonexistent in the natural environment. Natural water is a dynamic chemical system composed of a

complex group of gases, minerals and organic substances. All components contained in natural waters give them certain properties—salinity, alkalinity, hardness, acidity, etc. Knowledge of water chemical composition and its properties is required to understand these matrix chemical effects on adsorption using biochar.

Mineral substances contained in natural waters are dissolved as ions, complex ions, undissociated compounds and colloids. The major anions in natural water are Cl^-, SO_4^{2-}, HCO^{3-}, and CO_3^{2-} and the main cations are Ca^{2+}, Na^+, Mg^{2+}, and K^+. All natural waters contain dissolved gases but they differ in their origin. The composition of gases in natural waters depends mainly on their content in the atmosphere. Processes that take place in water bodies, including those that are biochemical, require the presence of oxygen (which is formed during photosynthesis), carbon dioxide, methane, and, to a lesser extent, hydrogen sulfide, ammonia, heavy hydrocarbons, and nitrogen. Some biogenous substances like silicon, nitrogen, phosphorous, and iron which are vital for aquatic organisms can also be found in water. It is therefore important to consider likely water matrix chemicals when evaluating the adsorptive properties of target metal ions with novel adsorbents.

2.3 Experimental

2.3.1 Reagents and equipment

All chemicals used were AR or GR-grade. Chemicals were purchased from Sigma-Aldrich (St. Louis, MO) unless specified. Stock solution (1000 mg/L) of lead was made by dissolving $Pb(NO_3)_2$ in de-ionized water from a Millipore-Q water system. The pH measurements were made using Hanna pH Meter (HI 2211) and the test solution pH was adjusted using HNO_3 (0.1 N) and NaOH (0.1 N). Adsorption studies were carried out

inside an Orbital shaker (Thermo Forma). The lead concentrations in the samples were determined using AAS (Shimadzu AA-7000). Stock solutions of Ca^{2+} (300 mg/L) and Mg^{2+} (100 mg/L) were made by dissolving $CaCl_2$ (0.414 g) and $MgCl_2$ (0.194 g) in de-ionized water (500 ml) from Millipore-Q water system. The Ca^{2+} and Mg^{2+} solutions were mixed in the ratio 2:1, respectively, to obtain hard water stock solutions (30 mg/L, 90 mg/L and 150 mg/L).

2.3.2 Biochar

Biochar (supplied by Biochar Supreme, Everson, WA) was produced as a by-product from the gasification of timber industry waste wood (Douglas fir). This biochar is designated as DBC (Douglas fir biochar) in this thesis. Auger fed, chipped (approximately 3 inches) green Douglas fir wood was introduced into an air-fed updraft gasifier at 900 – 1000 ºC with a residence time in the hot zone of about 1 s. Large biochar particles (~ 2 cm) were thoroughly washed several times with water to remove fine particulates, water soluble organic compounds, and other impurities. Then the particles were dried at room temperature. For this research, the biochar was ground, sieved to a particle size range of 150-300 µm and stored in closed vessels and used for all adsorption studies.

2.3.3 Preparation of magnetic biochar

The Douglas fir biochar was magnetized using the method described by Karunanayake et al.[45] Douglas fir biochar (DBC) (25 g, 150-300 µm diameter) was suspended in distilled water (250 ml). A ferrous sulfate solution was freshly prepared by adding 18.5 g (131.64 mmol) of $FeSO_4$ to distilled water (750 ml). A separate ferric

chloride solution was prepared by adding 9 g (110.97 mmol) $FeCl_3$ to 75 ml distilled water. Both the solutions were combined and stirred vigorously at 60-70 ºC for 5 min. The Fe^{2+}/Fe^{3+} solution formed was then added to the aqueous suspension of biochar at room temperature and slowly stirred for 30 min. After mixing, the pH of the Fe^{2+}/Fe^{3+}/DBC suspension was adjusted to between 10-11 using 10 M NaOH. The suspension was stirred for 60 min and aged at room temperature for 24 h, followed by filtration. The filtrate was washed with distilled water followed by ethanol. The washings ensure the removal of any remaining carboxylic acid, phenolic, and other acidic organic residuals from the biochar from the pyrolysis step. The resulting magnetized Douglas fir biochar (MDBC) was vacuum filtered and dried overnight at 50 ºC in a hot air oven.

2.3.4 Char characterization

2.3.4.1 Point of zero charge (PZC) measurement

The point of zero charge (PZC) of both DBC and MDBC was measured using 0.01 M NaCl aqueous solutions of pH 2, 4, 6, 8, and 10. The pH was adjusted using either 0.1 M NaOH or 0.1 M HCl solution. The solutions (25 mL) were brought into contact with 0.025 g of adsorbent and the system was stirred for 24 h. The supernatant was then decanted and the pH of the supernatant was measured using an ORION model 210 pH meter. The PZC was obtained by plotting pH of the initial solution against the pH of the supernatant.

2.3.4.2 Scanning electron microscopy (SEM) and energy dispersive analysis by X-ray (EDX)

Surface morphologies of both chars (DBC and MDBC) were examined using a scanning electron microscope model JEOL JSM-6500F FE-SEM at 5 kV. Samples were

mounted on a carbon stub using a double stick carbon tape. EDX analysis was carried out using a Zeiss, EVO 40 scanning electron microscope containing a BRUKER EDX system.

2.3.4.3 Transmission electron microscopy (TEM) and Energy-dispersive analysis by X-ray (EDX)

DBC and MDBC were analyzed with a JEOL model 2100 TEM operated at 200 kV. EDX was carried out using an Oxford X-max-80 detector. TEM samples were prepared by dispersing ~10 mg of char in 5 ml ethanol followed by 15 min of sonication. Each sample was then deposited onto a carbon coated copper grid and allowed to stand overnight prior to TEM/EDX analysis.

2.3.4.4 Surface area measurement

Surface area, micropore volume, and micropore diameter size of DBC and MDBC were measured by Brunauer-Emmet-Teller (BET) methods, using Micromeritics TriStar II Plus 3030 Analyzer and N_2 adsorption isotherms. Prior to each BET experiment, about 150 mg of sample was vacuum degassed at 180 °C for 1 h in the built-in degas port of the instrument.

2.3.4.5 Proximate analysis

Ash analysis was done for both chars by weighing the mass of ash produced from incinerating 1 g of the biochar in a muffle furnace in air at 1000°C for 15 h. The percentage of iron in MDBC sample was determined using atomic absorption spectroscopy (Shimadzu AA-7000) using iron standard solution (Sigma-Aldrich) for instrument calibration. An acid digestion was performed on 0.1 g of biochar using 50.0

mL of 1:1 95% H_2SO_4 /70% HNO_3. Iron from the biochar dissolved into the acid for 24 h with stirring and then was diluted with deionized water prior to atomic absorption spectroscopy analysis.

2.3.5 Sorption studies

Batch sorption studies were conducted to obtain rate and equilibrium data at different adsorbate concentrations to construct equilibrium isotherms. A known amount of biochar was added to 25 mL solutions containing different adsorbate concentrations in 40 ml amber glass vials. Samples were then agitated using the Orbital shaker for 60 min at 250 rpm. After equilibration, the samples were filtered through Whatman No. 1 filter paper. The amount of lead remaining in the filtrate was determined using atomic absorption spectroscopy (AAS) at λ_{max} wavelength of 283.3 nm. Samples were analyzed in triplicate and their average absorbances used. The amount of adsorbate removed per gram of adsorbent was obtained by:

$$q_e = \frac{V(C_0 - C_e)}{M} \quad (2.1)$$

where q_e is the amount of adsorbate (mg) removed per g of adsorbent, C_o and C_e are the initial and equilibrium adsorbate concentrations (mg/L) in solution, V is the solution volume (L), and M is the biochar weight (g).

2.3.6 Effect of water hardness on metal sorption

Batch sorption studies were conducted to study the effect of water hardness on rate and equilibrium data at different Pb^{2+} concentrations to construct equilibrium isotherms. Three levels of water hardness were employed; low (30 mg/L), medium (90 mg/L) and high (150 mg/L). A known amount of biochar was added to 25 mL solutions

containing different adsorbate concentrations prepared in these hard waters in 40 ml amber glass vials. Samples were then swirled for 60 min at 250 rpm and lead content analyzed as above.

2.3.7 Regeneration procedure

Used DBC and MDBC were recycled three times. Solutions (25 mL) containing 100 mg/L lead were equilibrated with 1 g/L of biochar, at pH 5 and 25°C. Desorption of lead from DBC and MDBC were carried out by washing with a total of 50 mL of 0.1 M HCl (5 × 10 mL for 10 min) followed by washing with water (10 mL) stirring for 10 min after each HCl treatment. Filtrates were analyzed by AAS.

2.4 Results and discussion

2.4.1 Characterization of biochar

SEM topography imaging was used to observe surface morphology of both DBC and MDBC. Figure 2.1 (A-C) shows the surface morphology of DBC and MDBC at high and low resolutions. These demonstrate porous surface that still contains much of the wood cells' original morphology. MDBC image shows morphological changes due to iron oxide impregnation inside the pores of the carbon matrix. After iron impregnation, a spongy porous texture is observed, suggesting the formation of well-dispersed iron oxide particles covering the MDBC. During magnetization some biochar pores could have been blocked or partially blocked by magnetite particles forming in the char.

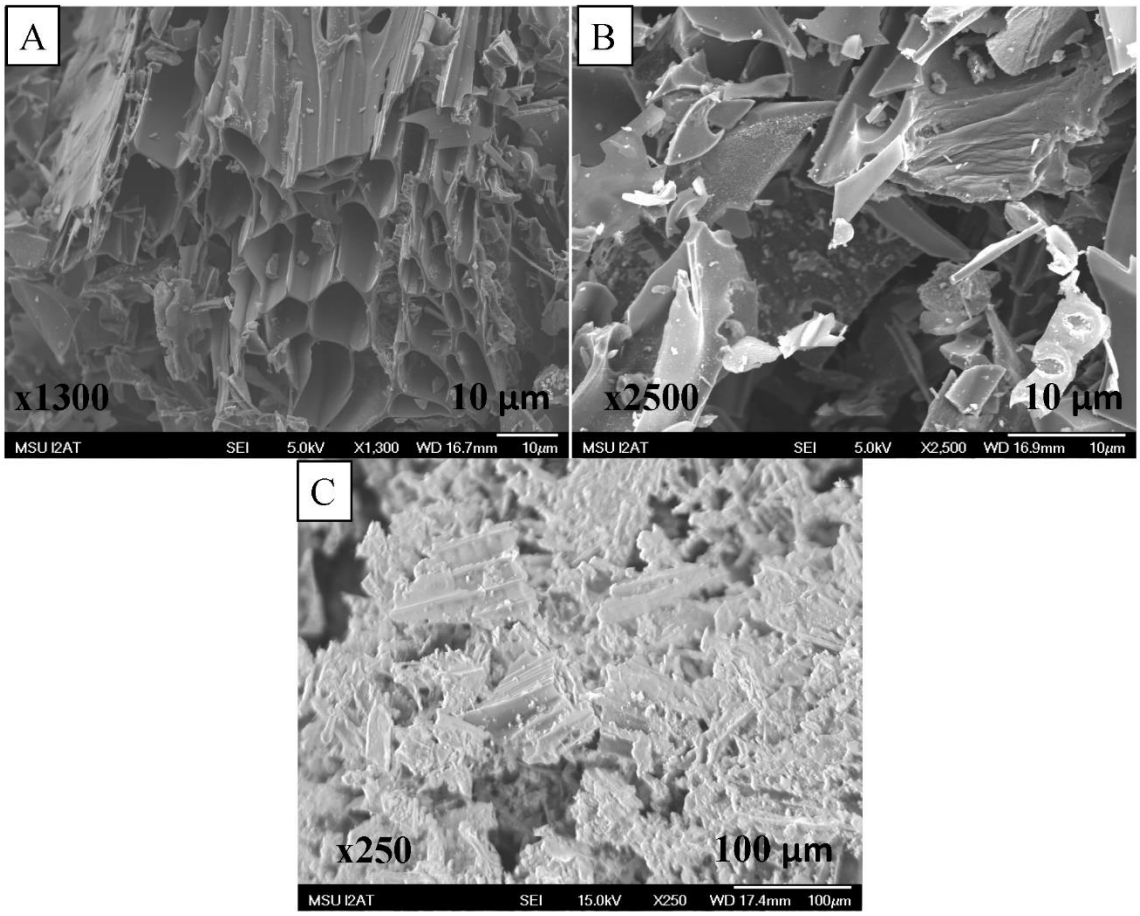

Figure 2.1 (A) and (B) are SEM images (different magnifications) of DBC and (C) shows the SEM image of MDBC

Morphological changes due to iron oxide particulate precipitation onto the char is clearly observed in image C.

Table 2.1 Elemental weight percentages from SEM-EDX analyses of DBC and MDBC

Elements	**DBC wt %**	**MDBC wt %**
Carbon	87.2	81.8
Oxygen	12.9	10.3
Iron	NA	7.9

The SEM-EDX determined elemental composition of the DBC and MDBC is shown in Table 2.1. Table 2.1 summarizes the weight percentage of different elements at different surface regions present on DBC and MDBC, respectively by SEM-EDX analyses. Iron loading is confirmed by the intense EDX iron peaks present in MDBC (7.9% Fe). These EDX iron peaks result from magnetite precipitation on the MDBC during the Fe^{3+}/Fe^{2+} treatment. EDX analyses cover specific areas of the surface and have limited depth of penetration. Since the surface regions are heterogenous at small scales, the %Fe by EDX is an approximation only of the surface composition and may not reflect bulk composition. Quantitative analysis of the total bulk sample percent iron (20.3%) of MDBC was determined using AAS.

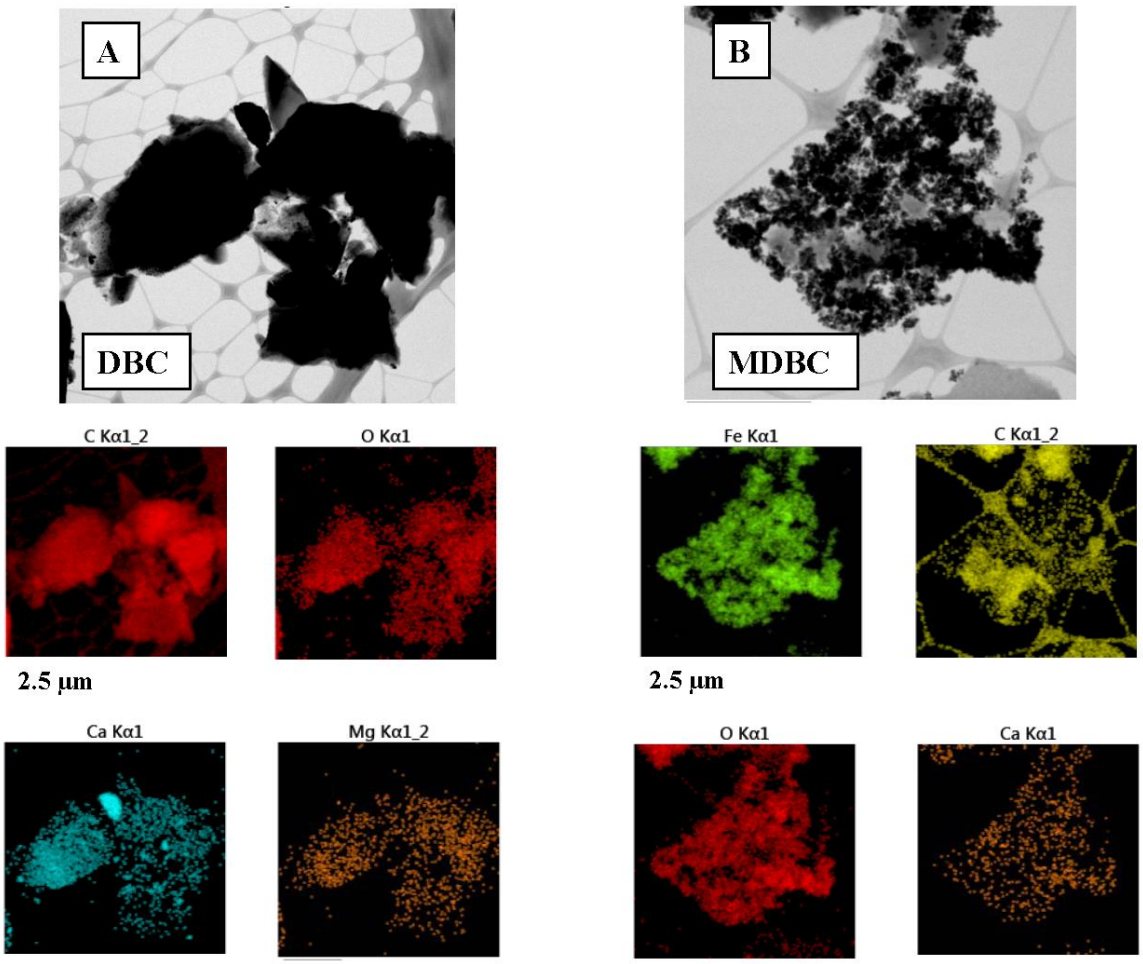

Figure 2.2 TEM images of (A) DBC and (B) MDBC

TEM-EDS maps show an even distribution of calcium and magnesium in DFB and that iron is evenly distributed in MDFB.

TEM analysis were conducted to examine iron oxide distribution before adsorption and to detect lead after adsorption on both DBC and MDBC (Figure 2.2). TEM-EDS maps (Figure 2.2) show abundant iron present on MDBC. TEM-EDS image of MDBC (Figure 2.2 (B)) clearly shows the overlapping distribution of iron and oxygen, supporting the existence of iron as an iron oxide.

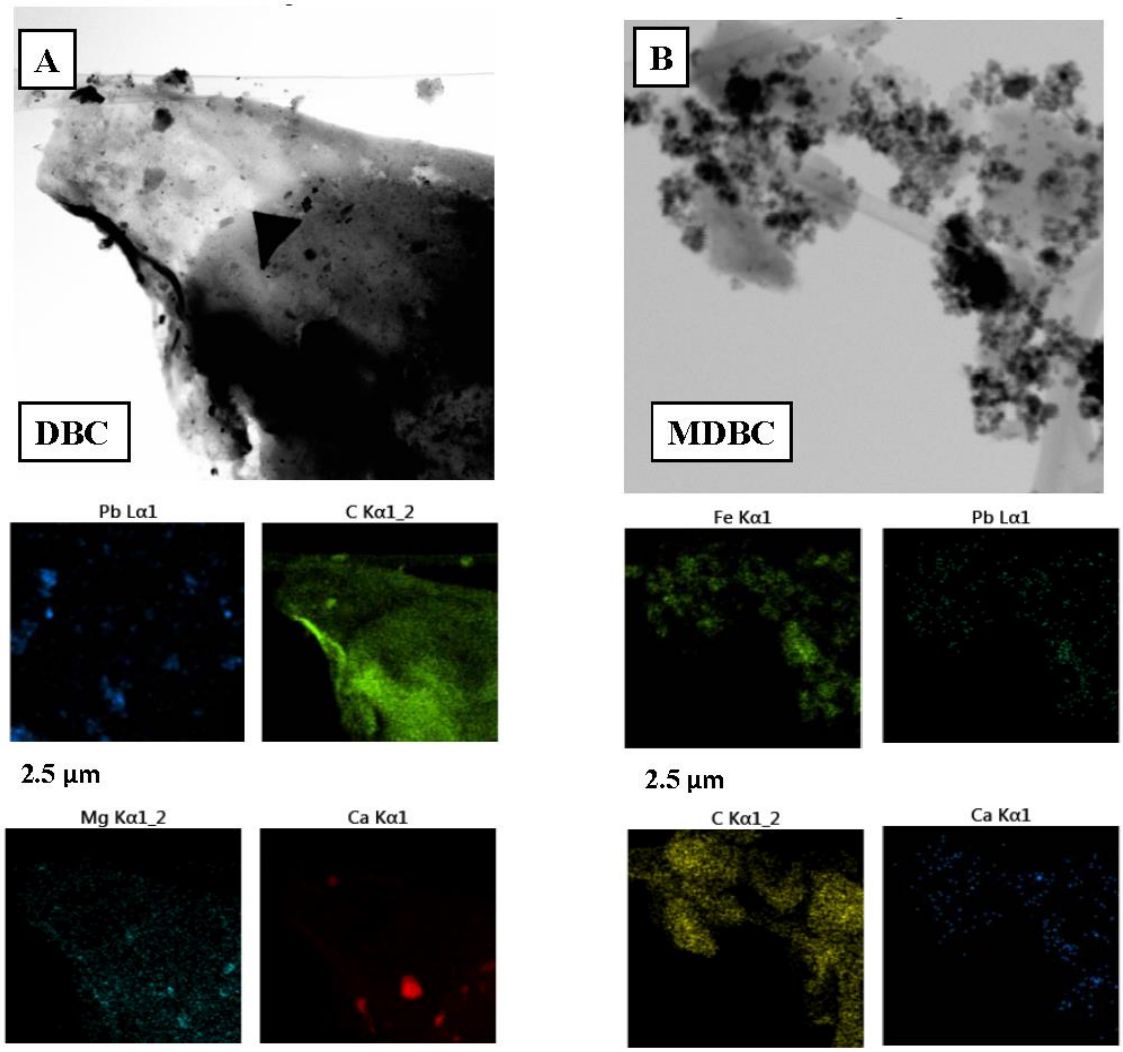

Figure 2.3 TEM images of (A) DBC after adsorption of lead and (B) MDBC after adsorption of lead onto each surface

Figure 2.3 display TEM- EDS images of DBC and MDBC after adsorption of lead (from solutions with Pb^{2+} concentration of 100 mg/L and an adsorbate concentration of 1 g/L). TEM-EDS maps show that lead is rather homogenously distributed over the DBC and MDBC surfaces. TEM-EDS elemental graphs (Figure 2.4) also confirmed the presence of iron on MDBC and that lead adsorption occurred onto both DBC and MDBC.

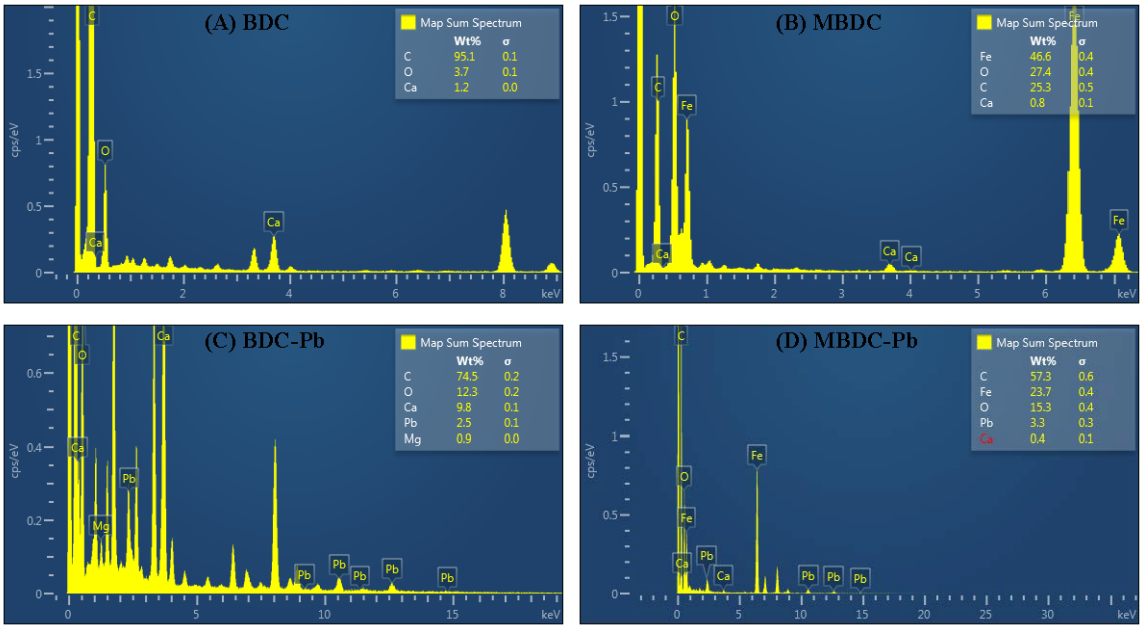

Figure 2.4 TEM-EDS element graphs of (A) DBC, (B) MDBC, (C) after adsorption of Pb^{2+} onto DBC and (D) after adsorption of Pb^{2+} onto MDBC

Metal concentration was 100 mg/L and the adsorbent concentration was 1 g/L.

Biochar magnetization results in higher Fe and ash content because the deposited iron oxides end up in the ash. The high surface area and pore volume of the DBC is the result of unusually high temperature (900-1000 °C) and fast residence time (about 1 s) employed in this biochar's production process. After magnetization, these values are somewhat reduced due to the deposition of iron oxide particles in and on the biochar pore surfaces. The surface morphology with large average pore sizes and large internal pore volumes of DBC and MDBC were large which encourages rapid water penetration into these biochars. The low density of the DBC and MDBC biochars allows for easy access of contaminated water, resulting in the extremely fast adsorption of Pb^{2+} and rapid establishment of adsorption equilibria.

Table 2.2 Surface areas, pore volumes, pore sizes, ash content, and iron weight percent (from AAS) of DBC and MDBC

Biochar Sample	**DBC**	**MDBC**
Surface area (m^2/g)	684	598
Pore volume (cm^3/g)	0.355	0.494
Pore size (Å)	21.4	32.7
Fe (% wt)	ND	20.3
Ash (% wt)	6.8	34.9

The point of zero charge (PZC) for DBC was ~10.06 and MDBC was ~8.03. The high temperatures (900-1000°C) used in the DBC production process and a Douglas fir feed stock with high mineral content (Ca^{2+} and Mg^{2+}) both contribute to the high PZC value for DBC. Calcium and magnesium contents were confirmed by TEM-EDS maps (Figure 2.2), all evidence suggests $CaCO_3$ and $MgCO_3$ are present in the surface region. Calcium and magnesium ions can react with carboxyl groups on the biochar surface and produced insoluble carbonate salts.[46] At the high temperatures used in the biochar production, carboxylic acids decarboxylate, lowering the acidity of DBC surface while the metal carbonates formed increase the PZC of DBC. The PZC drops from ~10.06 to ~8.03 following magnetization by Fe_3O_4 precipitation onto biochar surface producing the less basic MDBC because of removal of metal carbonates.

2.4.2 Sorption studies

2.4.2.1 Effect of solution pH on metal adsorption

Pb^{2+} uptake versus pH studies on DBC and MDBC were conducted in the pH range of 2-7 at 25 ºC and at adsorbate doses of 1g/L (Fig.2.5). An initial 50 ppm Pb^{2+} concentration was employed. Pb^{2+} adsorption by both chars was pH dependent. The greatest adsorption occurred at high pH values. The uptake of Pb^{2+} onto DBC increased from ~ 10 to 90% and for MDBC from ~ 9 to 64% as pH rises from 2 to 7. Aqueous Pb^{2+} ions undergo hydrolysis, solvation and polymerization above pH 7 which can lead to lead hydroxides precipitating and competition with adsorption. Hence, despite very fast adsorption equilibrium on DBC and MDBC, the pH 7 values on Figure 2.5 for Pb^{2+} could represent some competition from precipitation.

Pb^{2+} forms several hydrolysis products, which exist in different amounts under different conditions. In dilute solutions, Pb^{2+} hydrolysis products form at pHs > 6. The amount of Pb^{2+} adsorption is very low at initial pH values ~2-3 and then increases to 90% within the next 3 pH units. At pH > 6, Pb^{2+} removal from water took place both by adsorption and precipitation caused by hydroxyl ions present in water forming $Pb(OH)_2$ (s).

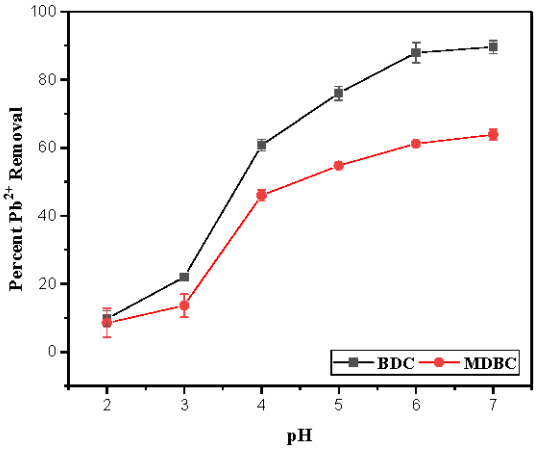

Figure 2.5 Effect of solution pH on Pb^{2+} adsorption on DBC and MDBC

Lead concentration was 50 ppm; total volume was 25 mL, mass of DBC and MDBC used were 0.025 g; standard deviation error bars are from 3 replicates.

The biochar surface functional groups can protonate or deprotonate with pH changes. Magnetized biochar also has Fe_3O_4 with surfaces that change with pH over the pH range from 2 to 7. In this range, lead will be present as 2+ ions. DBC has a higher adsorption capacity than MDBC at all pHs for both metals (Figure 2.5). The point of zero charge for DBC is ~10.06. So, going from pH 10.06 to 2, the DBC surface will be increasingly positive. Thus, at lower solution pH values, the positive DBC surface will tend to repel positively charged Pb^{2+}. As solution pH rises from 2 to 7, deprotonation of the biochar surface carboxylic acids and other acidic hydroxyl groups leads to lower net positive charge repulsions on the DBC surface, promoting metal cation attraction at negative locations. Thus, adsorption increases as pH rises.

MDBC is approximately 20 wt% iron with the remaining 80 wt% comprised of the original biochar. This lowers the original DBC surface area 684 m^2/g to 597 m^2/g for MBC. This likely contributes to the higher adsorption given by DBC versus MDBC.

MDBC will have the similar biochar functional groups as DBC, with its additional iron oxide surfaces. The surface of the iron oxide particles is terminated with iron bound hydroxyl groups. According to Cornell and Schwertmann, magnetite can form $FeOH^+$, $Fe(OH)_2^0$ and $Fe(OH)_3^-$ surface functions depending on pH.[47] The acid dissociation constant, pK_{a1} of magnetite is ~5.6. Below pH 5.6, Fe^{2+} and $FeOH^+$ are the dominant surface functional groups.[47-48] These positive sites can repel the positive Pb^{2+}. This leads towards lower adsorption at low pH for MDBC vs DBC along with MDBC's lower surface area. At high pH, the dominant functional groups of the iron oxide surface would be $Fe(OH)_2^0$ and $Fe(OH)_3^-$. The decrease in surface positive charges facilitates Pb^{2+} adsorption as pH rises.

2.4.2.2 Comparing adsorption verses contact time

Adsorption of Pb^{2+} uptake vs contact time was determined for DBC and MDBC from 1 min to 60 min in both distilled water (Figure 2.6) and water of low, medium and high hardness (Figure 2.7 and 2.8). The initial lead uptake rate on both biochars in distilled water is quite rapid. Typically, 60% of adsorption occurred within 15 min of contact. DBC with higher surface area (684 m^2/g) had the adsorption capacity of 50 mg/g as compared to MDBC (597 m^2/g) with the capacity of 43 mg/g under same conditions. Both DBC and MDBC reached equilibrium with lead within 45 min.

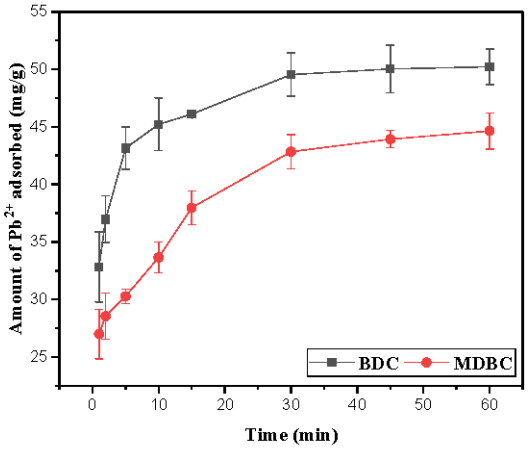

Figure 2.6 Comparison of rate, equilibrium times, and amount of Pb^{2+} adsorbed at pH 5 and 25 ºC on DBC and MDBC

Lead concentration was 50 mg/L; total volume was 25 mL, mass of each adsorbent used was 0.025 g.

Adsorption capacities vs contact time were also determined for lead in three different levels of water hardness. BDC had lead uptake of 48 mg/g, 47 mg/g and 43 mg/g for low, medium and hard water respectively. MDBC had lead uptake of 40 mg/g, 37 mg/g and 31 mg/g for low, medium and hard water respectively. As the level of hardness increases, the Pb^{2+} adsorption on biochar decreases. The decrease in the adsorption can be contributed to the fact that as hardness increases the concentration of Ca^{2+} and Mg^{2+} ions which compete with Pb^{2+} ions for the sorption sites.

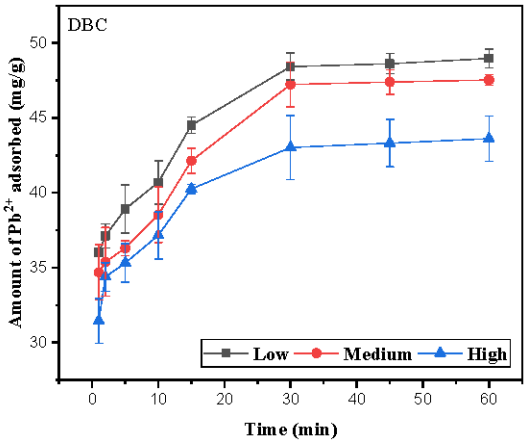

Figure 2.7 Comparison of rate, equilibrium times, and amount of Pb^{2+} adsorbed at pH 5 and 25 ºC on DBC in low, medium and high hardness water

Lead concentration was 50 mg/L; total volume was 25 mL, mass of each adsorbent used was 0.025 g.

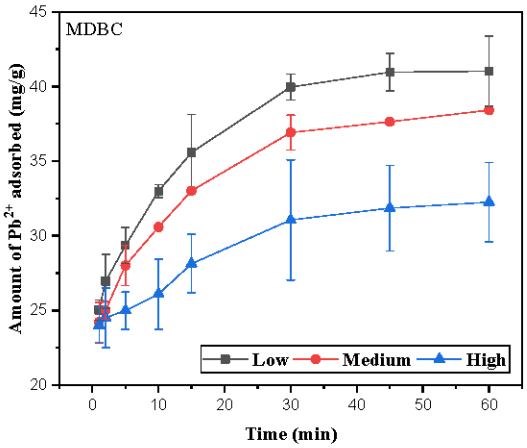

Figure 2.8 Comparison of rate, equilibrium times, and amount of Pb^{2+} adsorbed at pH 5 and 25 ºC on MDBC in low, medium and high hardness water

Lead concentration was 50 mg/L; total volume was 25 mL, mass of each adsorbent used was 0.025 g.

2.4.2.3 Effect of water hardness on Pb^{2+} sorption

Experimental results concerning the effect of water hardness on Pb^{2+} adsorption for both DBC and MDDC are presented in the Fig. 2.9 and 2.10. Three levels of water hardness were employed; low (30 mg/L), medium (90 mg/L) and high (150 mg/L). As water hardness increased from 0 mg/L of to 150 mg/L, the amount of lead adsorption on biochar decreased by 15 % for DBC and 21 % for MDBC.

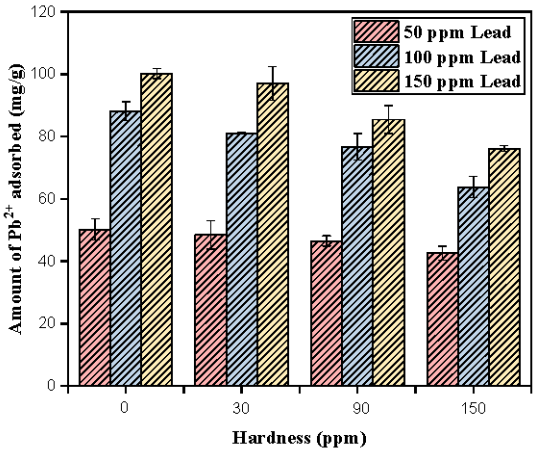

Figure 2.9 Comparison of amount of Pb^{2+} adsorbed (mg/g) as a function of water hardness on DBC

Total volume was 25 ml, DBC dose of 1 g/L, standard deviation error bars are from 3 replicates.

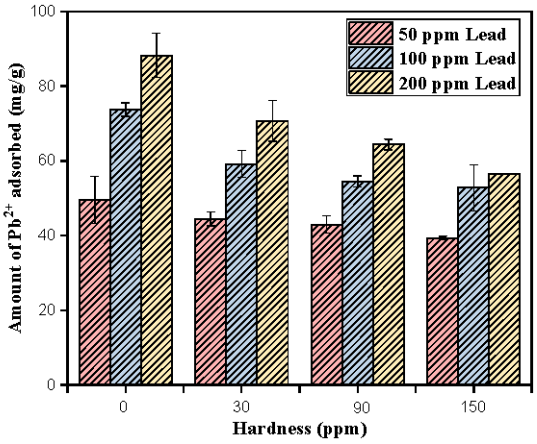

Figure 2.10 Comparison of amount of Pb^{2+} adsorbed (mg/g) as a function of water hardness on MDBC

Total volume was 25 ml, MDBC dose of 1 g/L, standard deviation error bars are from 3 replicates.

2.4.2.4 Sorption equilibrium studies and modelling as a function of water hardness

Lead sorption equilibrium studies at 25 ºC were conducted on both DBC and MDBC at pH 5 in low, medium and high hardness water. The initial Pb^{2+} concentration range was 50-250 mg/L and the equilibrium time was 60 min. Sorption equilibrium data were fitted to the two parameter Langmuir and Freundlich equations.[49-50] These models and related equations are summarized in the supporting information, Table A.1 (Appendix A). The parameters from all the models were evaluated using nonlinear regression (Origin 2016 software). The Langmuir and Freundlich two parameter models gave better fits ($R^2 > 0.99$) (Table 2.3). Figure 2.11 shows the Langmuir adsorption isotherm plots of the Pb^{2+} adsorbate, and these were used to calculate maximum monolayer adsorption capacities (Q^0 (mg/g)) at 25 ºC. Langmuir adsorption capacities on DBC, at pH 5, at 25 °C, and in low, medium and high harness water is 107, 86 and 77

mg/g. The adsorption capacities on MDBC in the hardness water are 70 mg/g, 65 mg/g and 63 mg/g. When considering the low potential cost of DBC and MDBC and its exceptionally rapid uptake rates, this adsorbent is very promising.

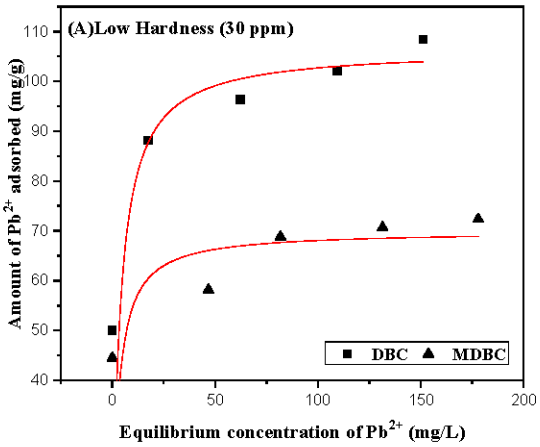

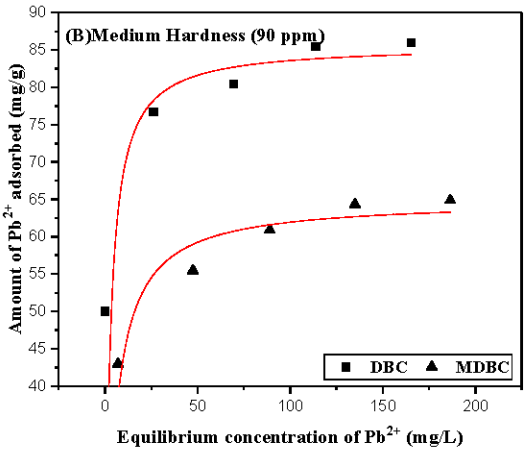

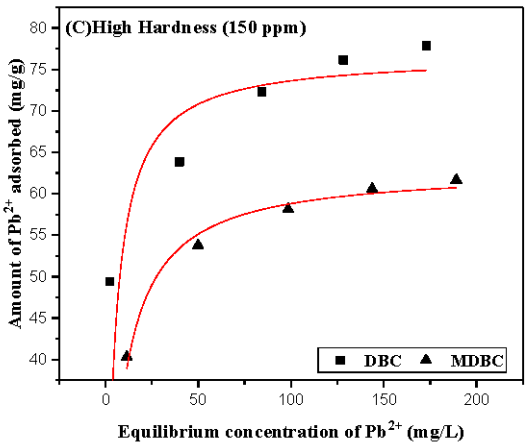

Figure 2.11 Langmuir adsorption isotherms for Pb^{2+} adsorption in (A) Low hardness water, (B) Medium hardness water and (C) High hardness water on both DBC and MDBC at 25 ºC

Lead concentration was 50-200 mg/L; adsorbent concentration 1 g/L and pH 5

Table 2.3 Langmuir and Freundlich isotherm parameters for lead removal on DBC and MDBC as a function of water hardness

Isotherm parameters		**DBC**			**MDBC**	
Hardness	Low	Medium	High	Low	Medium	High
Langmuir						
Q^0 (mg/g)	107	86	77	70	65	63
b	0.27	0.40	0.24	0.36	0.21	0.14
R^2	0.9965	0.9982	0.9956	0.9937	0.9987	0.9997
Freundlich						
K_f (mg/g)	67	62	42	40	34	30
1/n	0.09	0.07	0.12	0.12	0.13	0.16
R^2	0.9993	0.9998	0.9996	0.9982	0.9998	0.9995

2.4.2.5 Desorption and recovery of lead from DBC and MDBC

Desorption and recovery studies were determined by three adsorption and desorption cycles, after adsorption onto both DBC (Figure 2.12 (A)) and MDBC (Figure 2.12 (B)) from solutions (50 mL) using initial adsorbate concentrations of 100 mg/L for lead. DBC and MDBC doses of 0.05 g were added into 50 mL metal solutions at pH 5 and 25 °C. HCl (0.1 M) aqueous solutions were used for stripping. HCl was previously used to successfully strip Pb^{2+} from energy cane biochar.[51] Lead is soluble in HCl. At low pH, both protons and Pb^{2+} metal ions compete with biochar negative sites and with Fe-OH and FeO^- sites on iron oxide surface. Lead adsorption on DBC (Figure 2.12 (A)) decreased from 83% in the first cycle to 80% and 75%, respectively, in the second and third cycles. Notably, the amount of lead that was desorbed from DBC in the first cycle

was substantially less than that which had been initially adsorbed. The portion that did not desorb seems to be tightly held onto the biochar. During the second and third cycles, the fraction of metal desorbed, decreases for DBC. The amount of tightly held Pb^{2+} on MDBC is less than that on DBC, due to the lower biochar surface area of MDBC. Lead adsorption from MDBC (Figure 2.12 (B)) also decreased in each cycle (58 > 56 > 53% for Pb^{2+}). MDBC desorption is more complete with each cycle and the amount desorbed by MDBC is closer to the amount adsorbed.

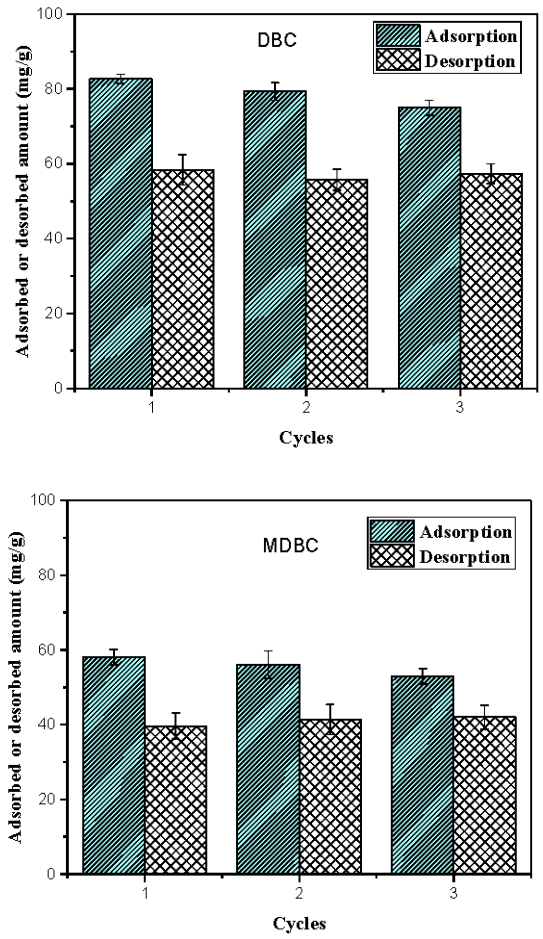

Figure 2.12 Adsorption-desorption cycles of Pb^{2+} from (A) DBC and (B) MDBC at 25 °C

An adsorbent amount of 1 g/L and an adsorbate concentration 100 mg/L for lead at pH 5 was used; desorption solvents were 0.1 M HCl (10 mL × 5) and water (10 mL).

2.4.2.6 Application of DBC and MDBC to environmental water samples

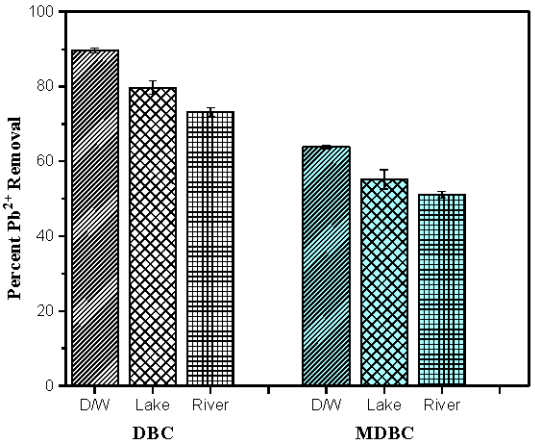

Figure 2.13 Comparison of adsorption of lead in distilled water, lake water and river water, at 25 ºC

Biochar doses of 1 g/L, metal concentration 100 mg/L, equilibrium time 60 min, error bars related to 3 replicates.

Natural water systems contain a complex mixture of ions that can interfere with Pb^{2+} during adsorption on DBC and MDBC. The efficiency of DBC and MDBC using authentic environmental water systems was investigated by collecting water from Oktibbeha County Lake, Starkville, Mississippi and the Pearl River, Neshoba County, Mississippi. The water samples were filtered through MF-Millipore (0.22 µm, GSWP04700) filter paper, followed by measurement of pH and water hardness (Table 2.4). The environmental water samples and distilled water sample (pH 5) were spiked with 100 mg/L of Pb^{2+} at 25 °C. DBC and MDBC doses of 0.025 g were then added to each of the 25 mL spiked water samples, followed by shaking for 60 min and analysis of the supernatant using AAS. Figure 2.13 compares the adsorption capacities for Pb^{2+} on both DBC and MDBC in the environmental water versus and distilled water. In lake

water, adsorption capacities of lead modestly decreased 11 % for DBC and 14 % for MDBC, versus their capacities in distilled water. In river water, adsorption capacities decreased by 18 % and 20 % onto DBC and MDBC, respectively. The decreased of adsorption capacity in natural water may be due to other interfering adsorbates.[51] This fall off is occurring despite the fact that the environmental waters have pH values where some precipitation might possibly add to the amount measured as adsorbed.

Table 2.4 Natural water parameters used for Pb^{2+} removal using BDC and MDBC

Natural waters	**pH**	**Hardness (ppm)**
Lake	6.92	40
River	7.35	50

2.5 Conclusion

Douglas fir fast pyrolysis biochar (DBC) was successfully converted to magnetic Fe_3O_4-modified Douglas fir biochar (MDBC). This was accomplished by chemical co-precipitation of iron-oxides onto the DBC. The chars were characterized for their BET surface area, proximate analysis and PZC. DBC had the high surface area, pore volume and pore size, versus MDBC. Surface morphology was studied using SEM and TEM. High solution pH was better for lead adsorption compared to low solution pH. Also, the equilibrium time for both DBC and MDBC was within 60 min. The unique production process used to make DBC results in high surface area and fast kinetics. Pb^{2+} adsorption is dependent on water hardness. As the hardness increases, the competition with calcium ions measurably reduces the absorbent affinity for lead. Sorption equilibrium studies

were conducted. The maximum Langmuir adsorption capacities in low, medium and high hardness waters are 107 mg/g, 86 mg/g and 77 mg/g on DBC and 70 mg/g, 65 mg/g and 63 mg/g on MDBC. Both Langmuir and Freundlich models gave better fits ($R^2 > 0.99$). The high uptake rate and high adsorption capacity features DBC would be suitable for continuous columns. MDBC would be advantageous for batch processes where magnetic removal would avoid slow filtration.

CHAPTER III

FUTURE WORK

3.1 Future work

The importance of heavy metal pollution control has increased significantly in last decades. The toxicity of heavy metals is a major concern. Therefore, there have been tremendous efforts on reducing their concentration in the environment. All the studies so far, on heavy metal adsorption by biochar have been carried out using distilled water. Using distilled water does not show the effects of competing adsorbates. This typically results in a high pollutant adsorption onto the biochar. As we have seen in this research, a 150 ppm increase in the hardness lowers lead adsorption by ~ 15%.

Other adsorbates present in natural waters compete for active sites on biochar and can lower the adsorption capacity for the substance of interest. Additional, related research is required including:

- Characterization of the effect of matrix chemicals found in natural waters on biochars' adsorption of lead. This would require a detailed analysis of the organic and inorganic components of specific natural water systems under study.
- Define how other heavy metals like cadmium, arsenic, chromium, etc. are also effected by water hardness in the same manner as Pb^{2+}.

- Monitoring the amount of Ca^{2+} and Mg^{2+} in the hard water solution before and after adsorption would also help in establish if these ions occupy active surface sites and reduce the adsorption capacity. Also, analysis of the adsorbent for competitors to Pb^{2+} adsorption should be performed.
- Expanding the above task to include additional organic and inorganic species commonly found in natural water systems.

REFERENCES

1. Karadede, H.; Ünlü, E., Concentrations of some heavy metals in water, sediment and fish species from the Atatürk Dam Lake (Euphrates), Turkey. *Chemosphere* **2000,** *41* (9), 1371-1376.

2. Konstantinou, I. K.; Hela, D. G.; Albanis, T. A., The status of pesticide pollution in surface waters (rivers and lakes) of Greece. Part I. Review on occurrence and levels. *Environmental Pollution* **2006,** *141* (3), 555-570.

3. Fawell, J.; Nieuwenhuijsen, M. J., Contaminants in drinking water. *British medical bulletin* **2003,** *68*, 199-208.

4. Daughton, C. G.; Ternes, T. A., Pharmaceuticals and personal care products in the environment: agents of subtle change? *Environmental Health Perspectives* **1999,** *107* (Suppl 6), 907-938.

5. Robinson, T.; McMullan, G.; Marchant, R.; Nigam, P., Remediation of dyes in textile effluent: a critical review on current treatment technologies with a proposed alternative. *Bioresource Technology* **2001,** *77* (3), 247-255.

6. Singh, V. K.; Bikundia, D. S.; Sarswat, A.; Mohan, D., Groundwater quality assessment in the village of Lutfullapur Nawada, Loni, District Ghaziabad, Uttar Pradesh, India. *Environmental monitoring and assessment* **2012,** *184* (7), 4473-88.

7. Barbir, F.; Veziroğlu, T. N.; Plass, H. J., Environmental damage due to fossil fuels use. *International Journal of Hydrogen Energy* **1990,** *15* (10), 739-749.

8. Rajput, S.; Pittman, C. U., Jr.; Mohan, D., Magnetic magnetite (Fe3O4) nanoparticle synthesis and applications for lead (Pb2+) and chromium (Cr6+) removal from water. *Journal of colloid and interface science* **2016,** *468*, 334-46.

9. Low, K. S.; Lee, C. K.; Liew, S. C., Sorption of cadmium and lead from aqueous solutions by spent grain. *Process Biochemistry* **2000,** *36* (1–2), 59-64.

10. Legret, M.; Pagotto, C., Evaluation of pollutant loadings in the runoff waters from a major rural highway. *Science of The Total Environment* **1999,** *235* (1), 143-150.

11. Basta, N. T.; Gradwohl, R.; Snethen, K. L.; Schroder, J. L., Chemical Immobilization of Lead, Zinc, and Cadmium in Smelter-Contaminated Soils Using Biosolids and Rock Phosphate Published with approval of the Director, Oklahoma Agric. Exp. Stn. *Journal of Environmental Quality* **2001,** *30* (4), 1222-1230.

12. Edwards, M.; Triantafyllidou, S.; Best, D., Elevated Blood Lead in Young Children Due to Lead-Contaminated Drinking Water: Washington, DC, 2001−2004. *Environmental Science & Technology* **2009,** *43* (5), 1618-1623.

13. Howard, P. H.; Muir, D. C. G., Identifying New Persistent and Bioaccumulative Organics Among Chemicals in Commerce. *Environmental Science & Technology* **2010,** *44* (7), 2277-2285.

14. Järup, L., Hazards of heavy metal contamination. *British medical bulletin* **2003,** *68* (1), 167-182.

15. Meunier, N.; Drogui, P.; Montané, C.; Hausler, R.; Mercier, G.; Blais, J.-F., Comparison between electrocoagulation and chemical precipitation for metals removal from acidic soil leachate. *Journal of Hazardous Materials* **2006,** *137* (1), 581-590.

16. Tavakoli, O.; Goodarzi, V.; Saeb, M. R.; Mahmoodi, N. M.; Borja, R., Competitive removal of heavy metal ions from squid oil under isothermal condition by CR11 chelate ion exchanger. *Journal of Hazardous Materials* **2017,** *334*, 256-266.

17. Sabry, R.; Hafez, A.; Khedr, M.; El-Hassanin, A., Removal of lead by an emulsion liquid membrane. *Desalination* **2007,** *212* (1), 165-175.

18. Jha, M. K.; Kumar, V.; Jeong, J.; Lee, J.-c., Review on solvent extraction of cadmium from various solutions. *Hydrometallurgy* **2012,** *111–112*, 1-9.

19. Kushwaha, J. P.; Srivastava, V. C.; Mall, I. D., Organics removal from dairy wastewater by electrochemical treatment and residue disposal. *Separation and Purification Technology* **2010,** *76* (2), 198-205.

20. Mohan, D.; Pittman Jr, C. U., Activated carbons and low cost adsorbents for remediation of tri- and hexavalent chromium from water. *Journal of Hazardous Materials* **2006,** *137* (2), 762-811.

21. Mohan, D.; Singh, K. P., Single- and multi-component adsorption of cadmium and zinc using activated carbon derived from bagasse—an agricultural waste. *Water Research* **2002,** *36* (9), 2304-2318.

22. Boonamnuayvitaya, V.; Chaiya, C.; Tanthapanichakoon, W.; Jarudilokkul, S., Removal of heavy metals by adsorbent prepared from pyrolyzed coffee residues and clay. *Separation and Purification Technology* **2004,** *35* (1), 11-22.

23. Liu, H.; Peng, S.; Shu, L.; Chen, T.; Bao, T.; Frost, R. L., Magnetic zeolite NaA: Synthesis, characterization based on metakaolin and its application for the removal of Cu2+, Pb2+. *Chemosphere* **2013,** *91* (11), 1539-1546.

24. Mohan, D.; Pittman Jr, C. U., Arsenic removal from water/wastewater using adsorbents—A critical review. *Journal of Hazardous Materials* **2007,** *142* (1–2), 1-53.

25. Roberts, K. G.; Gloy, B. A.; Joseph, S.; Scott, N. R.; Lehmann, J., Life Cycle Assessment of Biochar Systems: Estimating the Energetic, Economic, and Climate Change Potential. *Environmental Science & Technology* **2010,** *44* (2), 827-833.

26. Laird, D.; Fleming, P.; Wang, B.; Horton, R.; Karlen, D., Biochar impact on nutrient leaching from a Midwestern agricultural soil. *Geoderma* **2010,** *158* (3–4), 436-442.

27. Field, J. L.; Keske, C. M.; Birch, G. L.; DeFoort, M. W.; Cotrufo, M. F., Distributed biochar and bioenergy coproduction: a regionally specific case study of environmental benefits and economic impacts. *Gcb Bioenergy* **2013,** *5* (2), 177-191.

28. Rajapaksha, A. U.; Chen, S. S.; Tsang, D. C. W.; Zhang, M.; Vithanage, M.; Mandal, S.; Gao, B.; Bolan, N. S.; Ok, Y. S., Engineered/designer biochar for contaminant removal/immobilization from soil and water: Potential and implication of biochar modification. *Chemosphere* **2016,** *148*, 276-291.

29. Tan, X.; Liu, Y.; Zeng, G.; Wang, X.; Hu, X.; Gu, Y.; Yang, Z., Application of biochar for the removal of pollutants from aqueous solutions. *Chemosphere* **2015,** *125*, 70-85.

30. Mohan, D.; Sarswat, A.; Singh, V. K.; Alexandre-Franco, M.; Pittman Jr, C. U., Development of magnetic activated carbon from almond shells for trinitrophenol removal from water. *Chemical Engineering Journal* **2011,** *172* (2–3), 1111-1125.

31. Patzak, M.; Dostalek, P.; Fogarty, R. V.; Safarik, I.; Tobin, J. M., Development of magnetic biosorbents for metal uptake. *Biotechnology Techniques* **1997,** *11* (7), 483-487.

32. Kwapinski, W.; Byrne, C. M. P.; Kryachko, E.; Wolfram, P.; Adley, C.; Leahy, J. J.; Novotny, E. H.; Hayes, M. H. B., Biochar from Biomass and Waste. *Waste and Biomass Valorization* **2010,** *1* (2), 177-189.

33. Van Zwieten, L.; Kimber, S.; Morris, S.; Chan, K. Y.; Downie, A.; Rust, J.; Joseph, S.; Cowie, A., Effects of biochar from slow pyrolysis of papermill waste on agronomic performance and soil fertility. *Plant and Soil* **2010,** *327* (1), 235-246.

34. Gaunt, J. L.; Lehmann, J., Energy Balance and Emissions Associated with Biochar Sequestration and Pyrolysis Bioenergy Production. *Environmental Science & Technology* **2008,** *42* (11), 4152-4158.

35. Rafiq, M. K.; Bachmann, R. T.; Rafiq, M. T.; Shang, Z.; Joseph, S.; Long, R., Influence of Pyrolysis Temperature on Physico-Chemical Properties of Corn Stover (Zea mays L.) Biochar and Feasibility for Carbon Capture and Energy Balance. *PLoS ONE* **2016,** *11* (6), e0156894.

36. Jamradloedluk, J.; Lertsatitthanakorn, C., Characterization and Utilization of Char Derived from Fast Pyrolysis of Plastic Wastes. *Procedia Engineering* **2014,** *69*, 1437-1442.

37. Bach, Q.-V.; Tran, K.-Q., Dry and Wet Torrefaction of Woody Biomass – A Comparative Studyon Combustion Kinetics. *Energy Procedia* **2015,** *75*, 150-155.

38. Meyer, S.; Glaser, B.; Quicker, P., Technical, Economical, and Climate-Related Aspects of Biochar Production Technologies: A Literature Review. *Environmental Science & Technology* **2011,** *45* (22), 9473-9483.

39. Dong, X.; Ma, L. Q.; Li, Y., Characteristics and mechanisms of hexavalent chromium removal by biochar from sugar beet tailing. *J Hazard Mater* **2011,** *190* (1-3), 909-15.

40. Kumar, S.; Loganathan, V. A.; Gupta, R. B.; Barnett, M. O., An Assessment of U(VI) removal from groundwater using biochar produced from hydrothermal carbonization. *Journal of Environmental Management* **2011,** *92* (10), 2504-2512.

41. El-Shafey, E. I., Removal of Zn(II) and Hg(II) from aqueous solution on a carbonaceous sorbent chemically prepared from rice husk. *Journal of Hazardous Materials* **2010,** *175* (1–3), 319-327.

42. Mukherjee, A.; Zimmerman, A. R.; Harris, W., Surface chemistry variations among a series of laboratory-produced biochars. *Geoderma* **2011,** *163* (3–4), 247-255.

43. A review of biochar as a low-cost adsorbent for aqueous heavy metal removal. *Critical Reviews in Environmental Science and Technology* **2016,** *46* (4), 406-433.

44. Veluchamy, C.; Kalamdhad, A. S., Enhanced methane production and its kinetics model of thermally pretreated lignocellulose waste material. *Bioresource Technology* **2017,** *241*, 1-9.

45. Karunanayake, A. G.; Bombuwala Dewage, N.; Todd, O. A.; Essandoh, M.; Anderson, R.; Mlsna, T.; Mlsna, D., Salicylic Acid and 4-Nitroaniline Removal from Water Using Magnetic Biochar: An Environmental and Analytical Experiment for the Undergraduate Laboratory. *Journal of Chemical Education* **2016,** *93* (11), 1935-1938.

46. Yuan, J. H.; Xu, R. K.; Zhang, H., The forms of alkalis in the biochar produced from crop residues at different temperatures. *Bioresour Technol* **2011,** *102* (3), 3488-97.

47. Cornell, R. M.; Schwertmann, U., Transformations. In *The Iron Oxides*, Wiley-VCH Verlag GmbH & Co. KGaA: 2004; pp 365-407.

48. Chowdhury, S. R.; Yanful, E. K.; Pratt, A. R., Chemical states in XPS and Raman analysis during removal of Cr(VI) from contaminated water by mixed maghemite-magnetite nanoparticles. *Journal of Hazardous Materials* **2012,** *235-236*, 246-256.

49. Langmuir, I., THE ADSORPTION OF GASES ON PLANE SURFACES OF GLASS, MICA AND PLATINUM. *Journal of the American Chemical Society* **1918,** *40* (9), 1361-1403.

50. Freundlich, H., Over the adsorption in solution. *J. Phys. Chem* **1906,** *57* (385), e470.

51. Mohan, D.; Singh, P.; Sarswat, A.; Steele, P. H.; Pittman, C. U., Lead sorptive removal using magnetic and nonmagnetic fast pyrolysis energy cane biochars. *Journal of colloid and interface science* **2015,** *448*, 238-250.

APPENDIX A

SUPPORTING INFORMATION

Table A.1 Summary of isotherms used to fit experimental data

Model name	Equation	Description	Parameters	Ref.
Langmuir	$q_e = \frac{Q^0 b C_e}{1 + b C_e}$	This isotherm assumes a homogeneous surface, monolayer coverage and no interactions of the adsorbate with neighboring sites	Q^0 (mg/g)-monolayer adsorption capacity; q_e (mg/g)-solute amount adsorbed per unit weight; C_e (mg/L)-solute equilibrium concentration; b-constant related to net enthalpy of adsorption	34
Freundlich	$q_e = K_F C_e^{1/n}$	This isotherm is used in the low to intermediate adsorbate concentration range.	q_e (mg/g)-adsorption capacity; C_e(mg/L)-solute equilibrium concentration; K_F (mg/g)-constant indicative of the relative adsorption capacity of adsorbent (mg/g); $1/n$-a constant indicative of the intensity of the adsorption	35